

Improving the Coverage of Millimeter-Wave (mmWave) Cellular Networks using Device-to-Device Relays

Shuanshuan Wu, *Student Member, IEEE*, Rachad Atat, *Student Member, IEEE*,
Nicholas Mastronarde, *Senior Member, IEEE*, and Lingjia Liu, *Senior
Member, IEEE*

Abstract

The susceptibility of millimeter waveform propagation to blockages may largely restrict the coverage of mmWave signals. To overcome blockages, we propose to leverage two-hop device-to-device (D2D) relaying. Using stochastic geometry, we derive expressions for the downlink coverage probability of a relay-assisted mmWave cellular network when the D2D links (from relays to destinations) are implemented in either the mmWave or microwave band. For mmWave links, we derive the coverage probability using dominant interferer analysis while accounting for both blockages and beamforming gains. For microwave D2D links, with the Rayleigh fading assumption, we derive the coverage probability considering different path loss models for line-of-sight (LOS) and non-line-of-sight (NLOS) links. Numerical results suggest that the downlink coverage of a mmWave cellular network can be improved by enabling two-hop D2D relay transmissions. In most situations, microwave D2D relays achieve better coverage than mmWave D2D relays because microwave D2D links can be established under NLOS conditions; however, mmWave D2D relays achieve better coverage when the density of interferers is large because their antenna arrays reject interference from off-boresight directions and blockages eliminate interference from NLOS interferers.

Index Terms

Millimeter Wave, Cellular, D2D, coverage, stochastic geometry, Poisson point process.

S. Wu and N. Mastronarde are with the Dept. of Electrical Engineering, University at Buffalo, The State University of New York, Buffalo, NY 14260 USA (e-mail: {shuanshu, nmastron}@buffalo.edu).

R. Atat and L. Liu are with the Electrical Engineering and Computer Science Dept., University of Kansas, Lawrence, KS 66044 USA (e-mail: {rachad, lingjialiu}@itcc.ku.edu).

I. INTRODUCTION

MILLIMETER-WAVE (mmWave) communication is attracting considerable attention from the scientific community and regulators for its potential to fulfill the ever increasing demands for mobile broadband access [1]. In industry, the 3rd Generation Partnership Project (3GPP) has started a study item focusing on the performance and feasibility of wireless communication in the mmWave band (6-100 GHz) [2]. Moreover, in July 2016, the Federal Communications Commission (FCC) unanimously voted to open nearly 11 GHz of mmWave spectrum for 5G [3]. However, due to its weak diffraction ability and severe penetration loss, mmWave communication is highly susceptible to blockages. For example, measurements on mmWave propagation show that tinted glass and brick pillars have high penetration losses of 40.1 dB and 28.3 dB, respectively, at a frequency of 28 GHz [4]; while in indoor environments, mmWave links actually experience intermittent connectivity due to blockages from mobile human bodies [5]. In other words, the transmissions in mmWave networks have to largely rely on LOS paths, which makes the coverage holes pronounced.

A straightforward solution to overcome blockages in mmWave cellular networks is to deploy more mmWave BSs. Although mmWave systems are expected to leverage highly directional steerable beam antenna arrays to extend their transmission range and to reduce intercell interference from off-boresight directions [6], significant interference may still be experienced in dense BS deployments. For example, the signal-to-interference-plus-noise ratio (SINR) at a user equipment (UE) that is located in the line-of-sight (LOS) path of a directional beam from a neighboring BS may be severely degraded [7]. Evidently, the likelihood of this happening will increase with the BS density;¹ therefore, interference management/coordination may become challenging in dense mmWave networks.

Another promising approach to extend coverage in mmWave cellular networks is to allow an intermediate relay node to forward traffic from a BS to a destination UE, which has poor links to nearby BSs. Due to the potential to route around blockages, using two-hop relay transmissions can improve mmWave coverage. In general, the relay transmission could be completed in the mmWave or microwave spectrum, and a relay node can either be deployed by an operator (a so-called *infrastructure relay* in long term evolution (LTE) [8], [9]) or can be an idle UE that

¹This intuition is verified in the analytical and simulation results in this report.

is used opportunistically. This latter case is attractive because it does not drastically change the network topology or infrastructure requirements. Since a UE serving as a relay connects to a destination UE via a device-to-device (D2D) link, we refer to it as a *D2D relay*.

D2D communications is already playing an important role in the unlicensed band via Wi-Fi Direct [10]. However, its counterpart in the licensed band is far from being fully developed. A preliminary version of D2D communications called Proximity Service (ProSe) [11] is standardized in Rel-12 LTE-Advanced; however, it is mainly targeted for public safety use [12]. Aside from enhancing public safety, D2D communications can improve spectral efficiency in microwave cellular networks up to $4 - 5\times$ [14]. Moreover, it opens up opportunities for social networking [16], multicasting [17], machine type communications [18], and D2D content distribution [15]. There is also work focusing on D2D communications in mmWave spectrum [26].

D2D relaying to extend network coverage for public safety use is introduced in Rel-13 LTE-Advanced [13], [32]. In [19], we address the problem of incentivizing UEs to relay in commercial cellular networks. Currently, there is only limited research on D2D relay-assisted mmWave cellular communications [27], [28]. In [27], multi-hop relaying is used to improve connectivity of mmWave networks. In cellular networks, however, using more than two hops may increase signaling overheads, scheduling delays, and interference. In [28], the authors investigate the relay selection problem in a two-hop relay-assisted mmWave cellular network based on obstacle analysis. However, it does not provide a systematic performance analysis of D2D relay-assisted mmWave cellular networks. In this report, we work toward filling this gap by analyzing the coverage probability of D2D relay-assisted mmWave cellular networks, where the D2D link operates in mmWave or microwave spectrum.

In conventional cellular network performance evaluations, BSs are usually assumed to be arranged in hexagonal or square grids and system performance is evaluated by simulation. However, grid models are known to be too ideal because actual BS deployments are restricted by terrain and obstacles. Another shortcoming of grid BS models is their lack of tractability. Recently, stochastic geometry has gained popularity as a powerful tool for modeling/evaluating wireless networks [22], [23] not only because it provides a mathematically tractable framework to do so, but also because positions of BSs in real networks often resemble point processes [30], [24], which are widely used in stochastic geometry.

In this report, we analyze the downlink performance of a two-hop relay-assisted mmWave cellular network using stochastic geometry. In stochastic geometry analysis, spatial locations of network nodes (BSs and UEs) and obstacles are modeled by averaging over all their potential topological realizations [22], thereby providing a tractable approach for analyzing network performance [24]. In the considered relay-assisted mmWave cellular network, a downlink transmission is switched from direct cellular mode to D2D relay mode if there is an outage of the cellular link, but a relay UE is available that can help complete the transmission from the BS to the destination UE. For D2D transmissions (from relay UEs to destination UEs), both mmWave and microwave D2D relays are possible options. Intuitively, mmWave D2D is likely to achieve higher data rates due to the increased bandwidth available in the mmWave band, while microwave D2D may achieve better coverage in dense blockage scenarios because of the better propagation properties in the microwave band. Therefore, we will study and compare both D2D relay schemes.

Based on the assumption of cylindrical obstacles distributed according to 2D homogeneous Poisson point process (PPP), we are able to derive the LOS probability, which plays an important role in our coverage analysis. We show that the downlink coverage probability of a relay-assisted mmWave cellular network depends on the coverage of the direct cellular and D2D links, which are independent when D2D is deployed as an underlay to the uplink cellular spectrum. We then derive the coverage probability by stochastic geometry-based analysis. To be more specific, the contributions of the report are as follows: 1) We derive the coverage probability of mmWave cellular and mmWave D2D links based on dominant interferer analysis considering blockages and beamforming gains obtained using square antenna arrays. We also derive the coverage probability under noise-limited assumptions. 2) We derive the microwave D2D link coverage probability using different path loss models for LOS and non-line-of-sight (NLOS) D2D transmissions. 3) We validate our analytical results on the coverage probabilities of cellular and D2D links against simulations based on 3GPP network configurations and channel models. We then explore the effect of different parameters on the coverage of relay-assisted mmWave cellular networks (i.e., SINR threshold, BS antenna array size, obstacle density, and BS density). Our results demonstrate that two-hop D2D relays can improve coverage across a variety of network configurations.

The remainder of this report is organized as follows. In Section II, we present the system model. In Section III, we model and derive the coverage probability for two-hop relay-assisted

mmWave communication using stochastic geometry. In Section IV, we present numerical results based on the theoretical analysis and simulations. We finally conclude in Section V.

II. SYSTEM MODEL

A. Geometric Assumptions

1) *Preliminaries:* In this report, we model the spatial locations of BSs, UEs, and obstacles as 2D homogeneous PPPs. A PPP defined in \mathbb{R}^2 is a random process in which the number of points Φ in a bounded Borel set $\mathcal{B} \subset \mathbb{R}^2$ has a Poisson distribution:

$$\mathbb{P}(\Phi(\mathcal{B}) = k) = \frac{\Lambda^k}{k!} e^{-\Lambda}, k = 0, 1, 2, \dots \quad (1)$$

where $\Lambda = \lambda v_2(\mathcal{B})$ is the expectation of the Poisson random variable for some intensity λ and $v_2(\cdot)$ denotes the Lebesgue measure in \mathbb{R}^2 . If λ is constant, the PPP is said to be homogeneous.

2) *Obstacles:* To model blockage effects, we have to make specific assumptions on the shapes of obstacles. Generally, obstacles in transmission environments are amorphous: in outdoor environments, obstacles include buildings (rectangular or polygonal), trees (spherical, cylindrical or conic), and hills (amorphous); while in indoor environments, human bodies (cylindrical) are common obstacles. In [27], [29], blockage effects of rectangular obstacles like buildings are investigated. In our analysis, however, we model obstacles as cylinders that are spatially distributed according to a 2D homogeneous PPP Φ_o with intensity λ_o . Furthermore, we assume that each obstacle x_i has independent and identically distributed radius $R_{x_i} \in [r_{\min}, r_{\max}]$ and height $H_{x_i} \in [h_{\min}, h_{\max}]$ with probability density functions (PDF) $f_R(r)$ and $f_H(h)$, respectively.

3) *BSs and UEs:* We model the distributions of BSs as a 2D homogeneous PPP Φ_b with intensity λ_b .² We assume that UEs are also distributed according to a 2D homogeneous PPP and that they are partitioned between active and idle UEs, where idle UEs are candidate relays. The candidate relay UEs can be determined by independent thinning on the set of all UEs. We use Φ_{cr} and λ_{cr} to denote the point process and intensity of candidate relay UEs, respectively. Since the BSs, candidate relay UEs, and obstacles form homogeneous PPPs, we focus our analysis on a typical destination UE (in either the cellular or D2D link), which we assume is located at the origin \mathbf{o} . This is permissible in a homogeneous PPP by Slivnyak's theorem [22].

²In Section IV, we compare our analytical results derived based on the assumptions of a PPP against grid-based BS models.

B. MmWave Beamforming

As noted in the introduction, mmWave systems are expected to leverage highly directional beams to extend their transmission range [1], [20]. In this report, we consider a simple sectorized antenna array model for both mmWave transmitters and receivers [37]. In the mmWave cellular downlink, ϕ_b and ϕ_u (radians) denote the half-power beamwidths of BSs and UEs, respectively; the main lobe gain and side lobe gains of the BSs are denoted by Gm_b and Gs_b , respectively; and, for receiving UEs, the main and side lobe gains are denoted by Gm_u and Gs_u , respectively. With the assumption of an $N \times N$ uniform planar square antenna array with half-wavelength antenna spacing, the half-power beamwidth ϕ , main lobe gain G_m , and side lobe gain G_s are given as [21]

$$\phi = 1.732/N, \quad G_m = N^2, \quad G_s = 1/\sin^2\left(\frac{3\pi}{2N}\right). \quad (2)$$

The antenna array gain g_i from an arbitrary BS i at the typical cellular receiver is

$$g_i = \begin{cases} Gm_b Gm_u, & \text{with probability } \frac{\phi_b}{2\pi} \frac{\phi_u}{2\pi} \\ Gm_b Gs_u, & \text{with probability } \frac{\phi_b}{2\pi} (1 - \frac{\phi_u}{2\pi}) \\ Gs_b Gm_u, & \text{with probability } (1 - \frac{\phi_b}{2\pi}) \frac{\phi_u}{2\pi} \\ Gs_b Gs_u, & \text{with probability } (1 - \frac{\phi_b}{2\pi}) (1 - \frac{\phi_u}{2\pi}) \end{cases}. \quad (3)$$

For simplicity, we denote the four possible antenna gains in (3) as G_k , $k = 1, 2, 3, 4$. Note that the beamforming gain on the desired cellular link is always $g_0 = Gm_b Gm_u$; while g_i in (3) provides the possible antenna array gains from interferers. The interference antenna array gains on a D2D link can be acquired similarly. For tractability, we assume that an interfering transmitter's antenna boresight is uniformly distributed over $[0, 2\pi)$.

C. LOS Probability

As mentioned earlier, we model obstacles as cylinders that are spatially distributed according to a 2D homogeneous PPP Φ_o with intensity λ_o . We have the following conclusion regarding the LOS probability between two nodes.

Lemma 1 (LOS Probability). The LOS probability between two nodes separated by a distance d on the plane is

$$p_L(d) = \exp \left(- \lambda_o (2\mathbb{E}[R]d + \pi\mathbb{E}[R^2]) \right), \quad (4)$$

where λ_o is the obstacle intensity and the random variable R denotes the obstacle radius.

Proof. The proof is similar to the blockage analysis in [29] and is omitted to save space. ■

In the rest of this report, we will express the LOS probability defined in (4) as follows:

$$p_L(d) = ce^{-\beta d}, \quad (5)$$

where $c = e^{-\lambda_o \pi \mathbb{E}[R^2]}$ and $\beta = 2\lambda_o \mathbb{E}[R]$.

Note that Lemma 1 does not take obstacle height into consideration. However, BS antennas are typically mounted on roofs or towers to maintain LOS paths over short obstacles. To account for this, denote $H \in [h_{\min}, h_{\max}]$ the obstacle height with some PDF $f_H(h)$. It has been shown that the effective number of obstacles \hat{N} can be determined by thinning with a parameter η such that $\mathbb{E}[\hat{N}] = \eta \mathbb{E}[N]$, where N is the total obstacle number, and [29]

$$\eta = 1 - \int_0^1 \int_{h_{\min}}^{sH_{\text{Rx}} + (1-s)H_{\text{Tx}}} f_H(h) dh ds, \quad (6)$$

where H_{Tx} and H_{Rx} are the heights of the transmitter and receiver antennas, respectively. Note that η in D2D and cellular links may be different because they typically have different transmitter antenna heights. For clarity, the coefficient η for different link types will not be included in the following analysis; however, it will be taken into account in our numerical evaluations.

D. Channel Model

In this report, we consider the following path loss model for all link types (cellular and D2D) and for all spectrum bands (mmWave and microwave):

$$PL = A_1 \log_{10}(d) + A_2 + A_3 \log_{10}(f_c) + X \quad (\text{dB}),$$

where d (m) is the distance between the transmitter and receiver, f_c (GHz) is the carrier frequency, A_1 includes the path loss exponent, A_2 is the intercept, A_3 describes the path loss frequency

dependence, and X is an optimal environment-specific term, for example, it can be used to describe the wall attenuation. Path loss in linear scale can be expressed as $PL = A \cdot d^\alpha$, where $A = 10^{(A_2+X)/10} f_c^{A_3/10}$ and $\alpha = A_1/10$ is the path loss exponent. The values of A_1 , A_2 , A_3 and X depend on the deployment scenario. In the remainder of this report, we will use the notation A_L and A_N to differentiate the LOS and NLOS path loss.

We now describe the considered mmWave and microwave channel models in detail.

1) *MmWave Cellular and D2D Links*: Due to the properties of mmWave propagation, multi-path effects are negligible. For example, at 60 GHz, the channel closely matches an Additive White Gaussian Noise (AWGN) channel [7]. Consequently, we do not consider multi-path fading in our mmWave channel model. Interference experienced by a mmWave link comes from transmitters that have LOS paths to the receiver. On the downlink, interferers are BSs of neighboring cells. On the D2D link, interferers are uplink users and other D2D transmitters. Thus, the received signal power over a mmWave link of length d is

$$P_{Rx} = BP_{Tx}G_{Tx}G_{Rx}A^{-1}d^{-\alpha}, \quad (7)$$

where G_{Tx} and G_{Rx} denote the antenna array gains at the transmitter and receiver, respectively; P_{Rx} and P_{Tx} are the transmit and receive powers, respectively; and B is a Bernoulli random variable with

$$B = \begin{cases} 1, & \text{with probability } p_L(d), \\ 0, & \text{with probability } 1 - p_L(d). \end{cases} \quad (8)$$

2) *Microwave D2D Links*: Multi-path effects play an important role in microwave signal propagation. For tractability, we assume microwave D2D signals experience Rayleigh fading such that the instantaneous channel power gain h is exponentially distributed with PDF $f_h(x) = \mu e^{-\mu x}$, where $1/\mu$ is the average channel gain. Then, the normalized channel power gain has the unit exponential distribution ($1/\mu = 1$). In addition to Rayleigh fading, we consider both LOS and NLOS microwave signal propagation by using different path loss models for each case. Note that, in microwave communications, Rayleigh fading is most applicable when there is no dominant LOS path and Rician fading is typically used when there is a dominant LOS path. However, since large scale fading contributes significantly more to the signal power attenuation, we incorporate

the LOS/NLOS effect into the path loss model instead of complicating our analysis with Rician fading.³ The received power over a microwave D2D link with length d is modeled as

$$P_{\text{Rx}} = P_{\text{Tx}} h A^{-1} d^{-\alpha}. \quad (9)$$

Under LOS and NLOS path loss models, we replace α by α_{L} and α_{N} , respectively.

E. UE Association

To be consistent across the different types of links considered in this report (i.e., mmWave cellular, mmWave D2D, and microwave D2D), we assume that the receiver UE will always associate with the transmitter that has the smallest path loss. Here, “transmitter” refers to the mmWave BS (in cellular mode) or the relay UE (in D2D relay mode).

Since we assume that mmWave transmission is only possible when a LOS path exists, the above criterion indicates that the UE will always associate with the nearest LOS BS (in cellular mode) or the nearest LOS candidate relay UE (in mmWave D2D relay mode). Let $d_{0,L}$ denote the distance between a typical UE and the nearest LOS transmitter and let λ denote the intensity of candidate transmitters ($\lambda = \lambda_{\text{b}}$ for BSs and $\lambda = \lambda_{\text{cr}}$ for candidate relays). The PDF of $d_{0,L}$ is given in the following lemma.

Lemma 2 (PDF of the distance $d_{0,L}$). The PDF of the random variable $d_{0,L}$ is

$$f_{d_{0,L}}(d) = 2\pi\lambda d c e^{-\Lambda(d,\lambda) - \beta d}, \quad (10)$$

where $\Lambda(d, \lambda)$ is given as

$$\Lambda(d, \lambda) = \frac{2\pi\lambda c}{\beta^2} (1 - e^{-\beta d} - \beta d e^{-\beta d}). \quad (11)$$

Proof. The proof is provided in Appendix A. ■

For microwave D2D links, the typical UE will associate with the nearest LOS candidate relay UE or the nearest NLOS candidate relay UE, depending on which one provides the smallest path loss. Let $d_{0,N}$ denote the distance between the typical UE and the nearest NLOS candidate relay UE. The PDF of $d_{0,N}$ is given in the following lemma.

³We have validated this approximation in several scenarios under different parameter configurations against simulations using Rician fading. We omit these results due to space limitations.

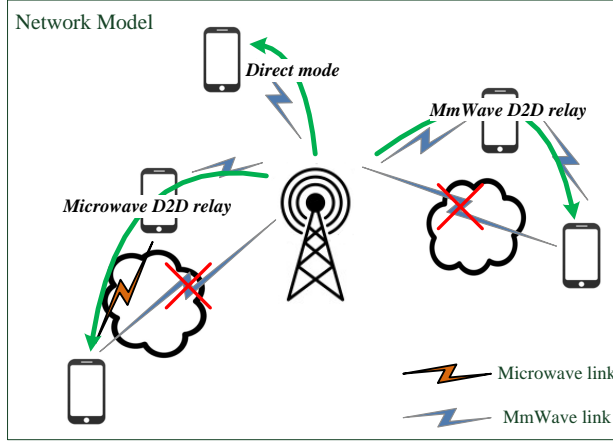


Fig. 1: Three transmission modes in the hybrid millimeter/microwave D2D relay-assisted cellular network: cellular/direct mode; mmWave D2D relay mode; and microwave D2D relay mode.

Lemma 3 (PDF of the distance $d_{0,N}$). The PDF of the random variable $d_{0,N}$ is

$$f_{d_{0,N}}(d) = 2\pi\lambda d(1 - ce^{-\beta d})e^{\Lambda(d,\lambda) - \pi\lambda d^2}, \quad (12)$$

where $\Lambda(d, \lambda)$ is defined in (11).

Proof. The proof is similar to the proof of Lemma 2 and is omitted to save space. ■

Based on the above discussion, operating in mmWave D2D relay mode requires the relay UE to have LOS paths to both the mmWave BS and the destination UE. On the other hand, to operate in microwave D2D relay mode, the relay UE must have a LOS path to the mmWave BS, but does not require a LOS path to the destination UE. Intuitively, the latter case may achieve better coverage due to the relaxed requirements on the relay UEs. The three transmission modes investigated in this work are shown in Fig. 1. Note that we consider D2D as an underlay to the uplink network, which means that D2D transmissions share the cellular system's uplink spectrum resources (i.e., uplink mmWave spectrum or uplink microwave spectrum).⁴ A list of frequently used notation is provided in Table I.

III. COVERAGE ANALYSIS

In the considered D2D relay-assisted cellular network, the downlink transmission switches from cellular to D2D relay mode when the direct cellular link (from the BS to the destination

⁴D2D as an underlay to the uplink spectrum is known to provide higher spectral efficiency than in the downlink spectrum because there is relatively lower interference in the uplink spectrum and it is often underutilized [32] [33].

TABLE I: List of abbreviated notation

Notation	Description
Φ_b, λ_b	PPP of BSs and its intensity
Φ_o, λ_o	PPP of obstacles and its intensity
Φ_{cr}, λ_{cr}	PPP of candidate relay UEs and its intensity
$p_L(x)$	LOS probability of a link with distance x
$p_c(T)$	Coverage probability with given outage SINR threshold T
$h, f_h(x)$	Fast fading channel power gain and its PDF
$R, f_R(r)$	Random variable of obstacle radius and its PDF
$H, f_H(x)$	Random variable of obstacle height and its PDF
$d_{0,L}, f_{d_{0,L}}(x)$	Distance from the typical UE to the nearest LOS transmitter and its PDF
$d_{0,N}, f_{d_{0,N}}(x)$	Distance from the typical UE to the nearest NLOS transmitter and its PDF
$\mathcal{B}(\mathbf{o}, d)$	A disc with radius d and centered origin \mathbf{o}

UE) experiences an outage and there exists an idle UE such that both the cellular link (from a BS to the idle UE) and the D2D link (from the idle UE to the destination UE) have SINRs above a threshold T . On the other hand, an outage occurs if the direct cellular link experiences an outage and such an idle UE does not exist. It follows that the downlink coverage probability (complementary outage probability) can be expressed as

$$p_c = 1 - (1 - p_{c,C})(1 - p_{c,R}),$$

where $p_{c,C}$ is the coverage probability of the cellular downlink, and $p_{c,R}$ is the probability that a two-phase D2D relay transmission is successfully set up. Because the cellular downlink and D2D transmissions are completed in orthogonal frequency bands, we model the coverage of each link as independent;⁵ therefore, $p_{c,R} = p_{c,C}p_{c,D}$, where $p_{c,C}$ is again the coverage probability of the cellular downlink and $p_{c,D}$ is the coverage probability of the D2D link. It follows that the downlink coverage probability in a D2D relay-assisted cellular network can be expressed as

$$\begin{aligned} p_c &= 1 - (1 - p_{c,C})(1 - p_{c,C}p_{c,D}) \\ &= p_{c,C}(1 + p_{c,D}) - p_{c,C}^2 p_{c,D}. \end{aligned} \tag{13}$$

We derive the coverage probability of the mmWave cellular downlink, $p_{c,C}$, in Section III-A. Subsequently, we derive the coverage probability, $p_{c,D}$, for mmWave D2D links in Section III-B and for microwave D2D links in Section III-D.

⁵Note that, in practice, cellular and D2D link coverage may be correlated because both links may be blocked by the same obstacle. For simplicity, we ignore this source of correlation; however, we will consider it in future work.

A. Coverage Probability of MmWave Cellular Links

Let $p_c(T) \triangleq \mathbb{P}(\text{SINR} > T)$ denote the coverage probability, where T is the outage SINR threshold. For a mmWave link, the desired signal at the receiver will experience interference if there is a LOS path to an interfering BS; however, the interference power depends on the distance and the antenna boresights of both the receiver and the interferer. Given a typical receiver, the SINR can be calculated as:

$$\text{SINR}_0 = \frac{g_0 A^{-1} d_0^{-\alpha}}{\sigma^2 + \sum_{i>0} B_i g_i A^{-1} d_i^{-\alpha}}, \quad (14)$$

where d_0 is the distance between the typical receiver and the serving BS, which is distributed according to the PDF in (10); d_i , $i > 0$, is the distance between the receiver and BS i ; and B_i is defined in (8). Note that, for brevity, we assume unit transmit power when defining the SINR.

As discussed earlier, a typical UE always associates to the nearest LOS BS, which has the smallest pathloss. Therefore, all other BSs with LOS paths to the typical UE are interferers that are farther from the typical UE than its associated BS. We partition these interferers into two subsets: *dominant* and *non-dominant* interferers [34]. A dominant interferer can cause an outage at the receiver, whereas a non-dominant interferer only contributes marginally to the interference.

Let $I = \sum_{i>0} B_i g_i A^{-1} d_i^{-\alpha}$ denote the aggregate interference at the typical receiver. Given the SINR outage threshold T and the distance d_0 between the typical UE and its nearest LOS BS, the coverage probability is defined as:

$$\begin{aligned} p_c(T, d_0) &= \mathbb{P}(g_0 A^{-1} d_0^{-\alpha} / (\sigma^2 + I) > T) \\ &= \mathbb{P}(I < (g_0 A^{-1} d_0^{-\alpha} - T \sigma^2) / T) \\ &\leq \mathbb{P}(d_i^{-\alpha} < (g_0 d_0^{-\alpha} - T A \sigma^2) / (g_i T)) \\ &= \mathbb{P}\left(d_i > (g_i T / (g_0 d_0^{-\alpha} - T A \sigma^2))^{1/\alpha}\right). \end{aligned} \quad (15)$$

In (15), the inequality follows from the fact that the third line only considers the interference from BS i rather than the aggregate interference. We denote by

$$D_1(T, d_0, g_i) = \left(\frac{g_i T}{g_0 d_0^{-\alpha} - T A \sigma^2} \right)^{1/\alpha},$$

a region around the typical UE where dominant interferers can exist. We refer to this bounded

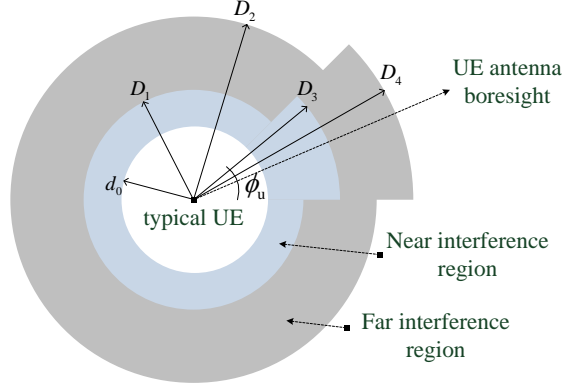


Fig. 2: Interference region with antenna array gain considered.

region as the *interference region (IR)*.

As we have seen in Section II-B, the antenna array gain g_i on an interfering link depends on the boresights of antenna arrays at both the interferer and the receiver, which means that the boundary of the IR varies with the direction. To be more specific, $D_1(T, d_0, g_i)$ can take four different values since there are four possible antenna array gains:

$$D_k = \left(\frac{G_k T}{g_0 d_0^{-\alpha} - T A \sigma^2} \right)^{1/\alpha}, \quad k = 1, 2, 3, 4, \quad (16)$$

where G_k is given in (3). An example IR is shown in Fig. 2. Note that, since interferers are farther than the serving BS, the IR actually excludes a disc $\mathcal{B}(\mathbf{o}, d_0)$ centered at the typical UE.

According to (16), we may further partition the IR into two parts: the *near interference region (NIR)* and the *far interference region (FIR)*. All LOS interferers in the NIR are dominant interferers; however, in the FIR, only LOS interferers with their main lobes towards the typical UE are dominant interferers. We thus have the following result for the coverage probability of a mmWave cellular link.

Theorem 1 (MmWave cellular coverage probability). Given the outage SINR threshold T , the coverage probability of a mmWave cellular link, $p_{c,c}(T)$, is given by

$$p_{c,c}(T) = 2\pi\lambda_b c \int_{x>0} x e^{-\Lambda_b^{(N)}(T,x) - \Lambda_b^{(F)}(T,x) - \Lambda(x,\lambda_b) - \beta x} dx, \quad (17)$$

where $\Lambda(x, \lambda_b)$ is defined in (11); and $\Lambda_b^{(N)}(T, x)$ and $\Lambda_b^{(F)}(T, x)$ are given as:

$$\begin{aligned}\Lambda_b^{(N)}(T, d_0) &= \frac{\lambda_b c}{\beta^2} \left(\phi_u (\beta d_0 e^{-\beta d_0} - \beta D_3 e^{-\beta D_3} + e^{-\beta d_0} - e^{-\beta D_3}) \right. \\ &\quad \left. + (2\pi - \phi_u) (\beta d_0 e^{-\beta d_0} - \beta D_1 e^{-\beta D_1} + e^{-\beta d_0} - e^{-\beta D_1}) \right), \\ \Lambda_b^{(F)}(T, d_0) &= \frac{\phi_b \lambda_b c}{2\pi \beta^2} \left(\phi_u (\beta D_3 e^{-\beta D_3} - \beta D_4 e^{-\beta D_4} + e^{-\beta D_3} - e^{-\beta D_4}) \right. \\ &\quad \left. + (2\pi - \phi_u) (\beta D_1 e^{-\beta D_1} - \beta D_2 e^{-\beta D_2} + e^{-\beta D_1} - e^{-\beta D_2}) \right),\end{aligned}$$

D_k , $k = 1, 2, 3, 4$ are given in (16).

Proof. The proof is provided in Appendix B. ■

Note that (17) provides an upper bound on the coverage probability of PPP-based model simulations because dominant interferer analysis uses a lower bound on the interference [see (15)]. It has been shown that this upper bound is tight in *ad hoc* networks [34]; yet, we may expect that the upper bound is even tighter in mmWave cellular networks because the LOS probability exponentially decreases with distance [see (5)] and the square antenna arrays reject interference from off-boresight directions, thereby reducing the effective number of distant interferers. We validate this in Section IV.

B. Coverage Probability of MmWave D2D Links

D2D links experience interference from other D2D transmissions and uplink cellular users. To account for this, we define a multiplexing factor ρ , which represents the average number of UEs transmitting on each sub-channel within a cell. For example, using orthogonal multiple access, $\rho \leq 1$, i.e., each sub-channel is used by at most one UE in each cell. Using orthogonal multiple access under a full buffer model (i.e., all UEs have data to transmit at all times), we have $\rho = 1$. For mmWave transmissions, ρ may be larger than 1 if there is sufficient separation of angles of arrival (AoA) and/or angles of departure (AoD) of concurrent D2D and/or uplink transmissions in the same sub-channel. Accounting for ρ , the interferers to a D2D link can be abstracted as a homogeneous PPP with intensity $\rho \lambda_b$. We have the following result for the coverage probability of a mmWave D2D link.

Theorem 2 (MmWave D2D coverage probability). Given the outage threshold T , the coverage probability of a mmWave D2D link, $p_{c,D}(T)$, is given as

$$p_{c,D}(T) = 2\pi\lambda_{cr}c \int_{x>0} x e^{-\Lambda_I^{(N)}(T,x) - \Lambda_I^{(F)}(T,x) - \Lambda(x,\lambda_{cr}) - \beta x} dx, \quad (18)$$

where $\Lambda_I^{(N)}(T, x)$ and $\Lambda_I^{(F)}(T, x)$ are given as:

$$\begin{aligned} \Lambda_I^{(N)}(T, d_0) &= \frac{\rho\lambda_b c}{\beta^2} \left(\phi_u (1 - \beta D_3 e^{-\beta D_3} - e^{-\beta D_3}) + (2\pi - \phi_u) (1 - \beta D_1 e^{-\beta D_1} - e^{-\beta D_1}) \right), \\ \Lambda_I^{(F)}(T, d_0) &= \frac{\phi_b \rho\lambda_b c}{2\pi\beta^2} \left(\phi_u (\beta D_3 e^{-\beta D_3} - \beta D_4 e^{-\beta D_4} + e^{-\beta D_3} - e^{-\beta D_4}) \right. \\ &\quad \left. + (2\pi - \phi_u) (\beta D_1 e^{-\beta D_1} - \beta D_2 e^{-\beta D_2} + e^{-\beta D_1} - e^{-\beta D_2}) \right), \end{aligned}$$

and D_k , $k = 1, 2, 3, 4$, is defined as in (16), but with G_k denoting the antenna array gain of the D2D link [similarly to (3)]; and $\Lambda(x, \lambda_{cr})$ is defined in (11).

Proof. The proof is similar to Theorem 1 and is thus omitted. ■

Note that the average number of interferers in the NIR, $\Lambda_I^{(N)}(T, d_0)$, is different than in the cellular link because interferers in D2D links may be arbitrarily close to the typical receiver.

C. Coverage Probability of Noise-Limited MmWave Links

Recent research suggests that mmWave networks are more likely to be noise-limited than interference-limited due to the blockage effect [35], [36]. A noise-limited mmWave link with length d_0 experiences an outage if the signal-to-noise ratio (SNR) at the receiver is below a given SNR outage threshold T . Therefore, the coverage probability is

$$p_c = \mathbb{P} \left[\frac{g_0 A^{-1} d_0^{-\alpha}}{\sigma^2} > T \right] = \mathbb{P} \left[d_0 < \left(\frac{g_0}{T A \sigma^2} \right)^{1/\alpha} \right] = F_{d_0}(x) \Big|_{x=\left(\frac{g_0}{T A \sigma^2}\right)^{1/\alpha}},$$

where $F_{d_0}(x)$ is the CDF of d_0 . In other words, the coverage probability of a noise-limited mmWave link is the probability that at least one transmitter (the BS in cellular mode or the candidate relay UE in D2D relay mode) with LOS path to the typical UE falls into the disc $B(\mathbf{o}, \left(\frac{g_0}{T A \sigma^2}\right)^{1/\alpha})$. We have the following result for the coverage probability of a noise-limited mmWave link.

Corollary 1 (Noise-limited mmWave coverage probability). For SINR threshold T , the coverage probability of a noise-limited mmWave link is

$$p_c(T) = 1 - \exp\left(-\frac{2\pi\lambda c}{\beta^2} \left(1 - e^{-\beta(\frac{g_0}{TA\sigma^2})^{1/\alpha}} - \beta(\frac{g_0}{TA\sigma^2})^{1/\alpha} e^{-\beta(\frac{g_0}{TA\sigma^2})^{1/\alpha}}\right)\right), \quad (19)$$

where λ is the transmitter intensity, i.e., $\lambda = \lambda_b$ for a cellular link and $\lambda = \lambda_{cr}$ for a D2D link.

We can see that, under the noise-limited assumption, the coverage probability of a mmWave link is largely simplified. In Section IV, we will evaluate the accuracy of the noise-limited assumption for both cellular and D2D links.

D. Coverage Probability of Microwave D2D Links

As in the Section III-B, we approximate the point process of interferers on the D2D link as a homogeneous PPP with intensity $\rho\lambda_b$, where ρ is the multiplexing factor. Additionally, we assume that the candidate relay UE with the smallest path loss is selected as the relay UE. Based on these two assumptions, we have the following result for the coverage probability of a microwave D2D link.

Theorem 3 (Microwave D2D coverage probability). Given the outage threshold T and candidate relay UE intensity λ_{cr} , the coverage probability of a microwave D2D link, $p_{c,D}(T)$, is given by

$$p_{c,D}(T) = S_N p_{c,N}(T) + S_L p_{c,L}(T), \quad (20)$$

where

$$S_L = 2\pi\lambda_{cr}c \int_0^\infty x e^{-\Lambda(x,\lambda_{cr}) - \beta x - \pi\lambda_{cr}\tilde{a}^2 x^{\frac{2\alpha_L}{\alpha_N}} + \Lambda(\tilde{a}x^{\frac{\alpha_L}{\alpha_N}},\lambda_{cr})} dx \quad (21)$$

is the probability that the typical UE associates with a LOS candidate relay UE, $S_N = 1 - S_L$ is the probability that the typical UE associates with a NLOS candidate relay UE, and $\tilde{a} = (A_L/A_N)^{1/\alpha_N}$. $p_{c,N}(T)$ and $p_{c,L}(T)$ are the coverage probabilities given that the nearest NLOS and nearest LOS candidate relay UEs are selected as a relays, respectively:

$$p_{c,N}(T) = 2\pi\lambda_{cr} \int_0^\infty x (1 - ce^{-\beta x}) e^{\Lambda(x,\lambda_{cr}) - \pi\lambda_{cr}x^2 - T\sigma^2 A_N x^{\alpha_N}} \mathcal{L}_I(TA_N x^{\alpha_N}) dx \quad \text{and} \quad (22)$$

$$p_{c,L}(T) = 2\pi\lambda_{cr}c \int_{x>0} e^{-\Lambda(x,\lambda_{cr}) - \beta x - T\sigma^2 A_L x^{\alpha_L}} \mathcal{L}_I(TA_L x^{\alpha_L}) dx, \quad (23)$$

where $\mathcal{L}_I(s)$ is the Laplace transform of the interference,

$$\mathcal{L}_I(s) = \exp \left(-\pi \rho \lambda_b s^{2/\alpha_N} \frac{2\pi/\alpha_N}{\sin(2\pi/\alpha_N)} \right). \quad (24)$$

Proof. The proof is provided in Appendix C. ■

Since NLOS UEs can serve as relays, we expect to achieve better coverage using microwave D2D relays than using mmWave D2D relays. In Section IV, we verify this observation.

IV. NUMERICAL RESULTS

In this section, we validate our analytical results against simulations based on 3GPP network evaluation methodologies, and explore the effect of different parameters on the coverage probabilities. In Section IV-A, we describe the simulation setup. In Section IV-B, we validate the derived coverage probabilities for the cellular and D2D links. In Section IV-C, we evaluate the noise-limited assumption. Finally, in Section IV-D, we investigate the coverage improvement by D2D relaying in different configuration assumptions.

A. Simulation Setup

We compare our analytical results against Urban Macro (UMa) and Indoor Office (Ind) 3GPP mmWave performance evaluation scenarios [2], and PPP-based network models. All of our simulations use the UE association strategy described in Section II-E in order to match our analytical results. Below, we describe our simulation setup in terms of the considered BS and UE distributions, obstacle distributions, antenna configurations, and channel models. Key simulation parameters are listed in Table II.

1) *BS and UE distributions:* In 3GPP's grid-based evaluation models, the UMa scenario has a hexagonal cell layout with inter-site distance (ISD) of 500 m. Meanwhile, the Ind scenario for mmWave evaluation has 12 BSs in a 50 m \times 120 m rectangular area, where each BS covers an area of size 25 m \times 20 m (Figure 7.2-1 in [2]). UEs are assumed to be randomly and uniformly dropped (which is essentially the same as 2D homogeneous PPP in implementation). For the PPP-based network models, the BSs are dropped according to 2D homogeneous PPPs with intensities $\lambda_b = 4.62 \times 10^{-6}/\text{m}^2$ and $\lambda_b = 2 \times 10^{-3}/\text{m}^2$ to match the average BS ISDs/densities in the 3GPP UMa and Ind scenarios, respectively. Additionally, UEs are assumed to be dropped

TABLE II: List of configuration parameters for performance evaluation

Parameters	UMa	Ind	Parameters	UMa	Ind
λ_b (BS/m ²)	4.62×10^{-6}	2×10^{-3}	BS antenna height (m)	25	3
Relay UEs per cell	10	3	BS Tx power (dBm)	35	24
R (uniform, m)	[20, 30]	[0.3, 0.6]	UE antenna height (m)	1.5	1
H (uniform, m)	[5, 25]	[1, 2]	UE Tx power (dBm)	23	23
η_C	0.5875	0.5	Noise power (dBm/Hz)	-174	-174
η_D	1	1	UE noise figure (dB)	9	9

according to a 2D homogeneous PPP. In both grid- and PPP-based network models, if there are n candidate relay UEs per cell on average, then the intensity of candidate relay UEs is $\lambda_{cr} = n\lambda_b$, where λ_b is the intensity of BSs.

2) *Obstacle distributions:* In the UMa and Ind scenarios, obstacles are mainly buildings and human bodies, respectively. We set the obstacle distribution parameters according to these considerations. The obstacle intensity $\lambda_o = \xi/(\pi\mathbb{E}^2[R])$ is determined by the expected obstacle radius $E[R]$ and the *obstacle cover ratio* ξ , i.e., the ratio of the area that is covered by obstacles ($0 < \xi < 1$). We assume that the obstacle radius R and height H are uniformly distributed on $[r_{\min}, r_{\max}]$ and $[h_{\min}, h_{\max}]$, respectively (see Table II). The LOS probability between two nodes is calculated using (5).

3) *Antenna configurations:* To model beamforming, we assume that mmWave transmitters and receivers are equipped with uniform planar antenna arrays. We consider BSs with $N_b \times N_b$ antenna arrays, with $N_b = 8$ and $N_b = 4$ (i.e. 64 and 16 transmit antenna ports, respectively). We assume that all UEs have 2×2 antenna arrays (i.e., 4 antenna ports) for both transmitting and receiving. Antenna array gains are determined according to (2). For example, the main lobe gain, side lobe gain, and beam width of a 4×4 array are 12.04 dB, 0.69 dB and 24.8° , respectively. We assume that microwave D2D links use a single transmit and receive antenna.

4) *Channel models:* A typical UE's coverage is determined by its received SINR and the outage threshold T . We use path loss models from 3GPP evaluation documents. For mmWave links, the LOS path loss models for the UMa and Ind scenarios are [2]:⁶

$$\begin{aligned}
 PL &= 32.4 + 20 \log_{10}(d) + 20 \log_{10}(f_c) \quad \text{and} \\
 PL &= 32.4 + 17.3 \log_{10}(d) + 20 \log_{10}(f_c),
 \end{aligned}$$

⁶In the path loss models defined in [2], the distance d is 3D distance, i.e., the transmitter and receiver antenna heights are considered. In this report, we use PPPs in \mathbb{R}^2 , so the distance is on the plain (2D).

respectively. For microwave D2D [39], the LOS and NLOS path losses for the UMa scenario are

$$PL_L = 27.0 + 22.7 \log_{10}(d) + 20 \log_{10}(f_c) \quad \text{and} \\ PL_N = 14.78 + 5.83 \log_{10}(1.5) + (44.9 - 6.55 \log_{10}(1.5)) \log_{10}(d) + 34.97 \log_{10}(f_c),$$

respectively, and in the Ind scenario are

$$PL_L = 89.5 + 16.9 \log_{10}(d/1000) \quad \text{and} \\ PL_N = 147.4 + 43.3 \log_{10}(d/1000),$$

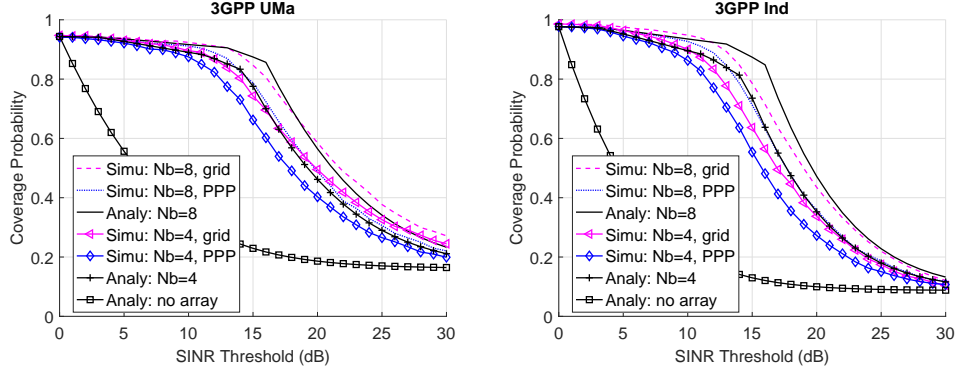
respectively. Note that d is in meters and f_c is in GHz. We set the carrier frequencies for mmWave and microwave links to 28 GHz and 2 GHz, respectively, and the mmWave and microwave link bandwidths to 100 MHz and 20 MHz, respectively.

To calculate the SINR in the mmWave simulations, the interference power from all effective LOS interferers is considered (in contrast to our analytical results, which only consider dominant interferers). To model the interference on D2D links, we set the multiplexing factor to $\rho = 1$. In other words, we consider a full buffer traffic model and assume that the BS schedules exactly one cellular UE or D2D UE on each uplink sub-channel at a given time.

B. Validation of Analytical Expressions

In this section, we compare our analytical results against the UMa and Ind 3GPP mmWave performance evaluation scenarios, and PPP-based network simulations, as described in Section IV-A.

1) *MmWave Cellular Link Coverage*: The coverage probabilities for the mmWave cellular links, obtained analytically from (17) (Theorem 1), are shown in Fig. 3 with respect to the SINR threshold and compared against the PPP- and 3GPP grid-based model simulations. For illustration, the obstacle densities, ξ , for the UMa and Ind scenarios are set to 0.2 and 0.08, respectively. In the Ind scenario, $\xi = 0.08$ means that there are 12 people (or other obstacles) in a 100 m² area on average. As expected, the analytical results obtained by dominant interferer analysis provide an upper bound on the PPP-based model simulations and the upper bound is relatively tight. This is because the LOS probability exponentially decreases with distance [see (5)] and the antenna arrays reject interference from off-boresight directions, thereby effectively reducing the number of distant interferers. We also observe that, for large SINR thresholds, the analytical results for the UMa scenario are bounded by the grid and PPP simulations. We



(a) 3GPP UMa (Analy & Grid Sims & PPP Sims). (b) 3GPP Ind (Analy & Grid Sims & PPP Sims).

Fig. 3: Validation of the mmWave cellular coverage probabilities in (17) (Theorem 1) with respect to the SINR threshold. Dominant interferer analysis provides a good approximation of the mmWave cellular coverage probability.

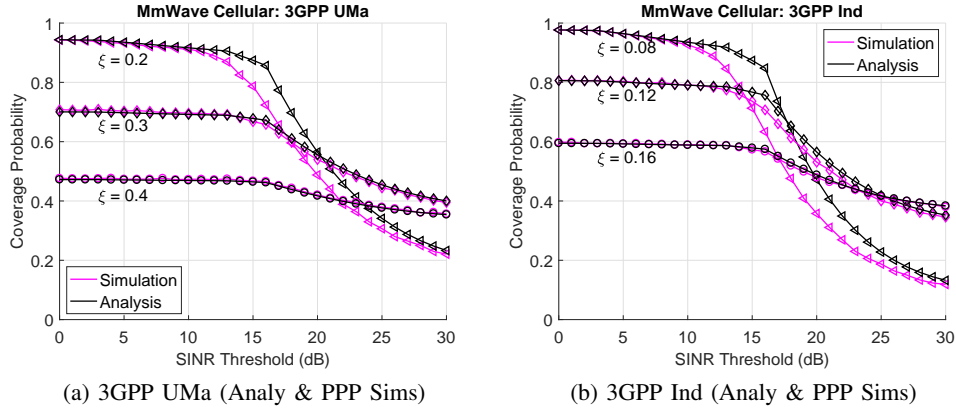


Fig. 4: Validation of the mmWave cellular coverage probabilities (17) (Theorem 1) with respect to obstacle densities against the PPP-based model simulations. Dominant interferer analysis provides more accurate results as the obstacle density increases (large ξ). Higher obstacle densities lead to higher coverage probabilities at high SINR thresholds.

conclude that the analytical coverage probability expression in (17) derived using dominant interferer analysis is a reasonable approximation in both 3GPP UMa and Ind scenarios.

In Fig. 3, we observe that the 8×8 antenna array achieves better coverage than the 4×4 array, which is due to the increased transmission distance and increased spatial isolation (and reduced interference) enabled by narrower beams. We also show the analytical coverage probability achieved when the antenna array is disabled. In this case, the coverage rapidly decreases as the SINR threshold increases. In the remaining evaluations, we default to the 8×8 antenna array.

In Fig. 4, we show the mmWave cellular coverage probabilities in (17) with respect to the SINR threshold for several obstacle densities. We can see that the analytical results obtained by dominant interference analysis become increasingly accurate as the obstacle density increases.

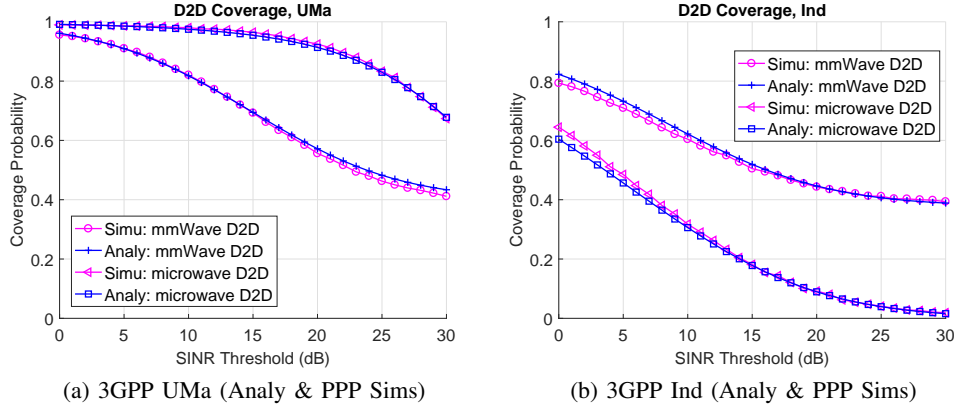


Fig. 5: Validation of the mmWave and microwave D2D link coverage probabilities in (18) (Theorem 2) and (20) (Theorem 3), respectively, against the PPP-based model simulations. Dominant interferer analysis for mmWave D2D links provides a tighter upper bound than for mmWave cellular links. Microwave D2D links achieve better coverage than mmWave D2D links in the UMa scenario; but in the Ind scenario, microwave D2D performs worse than mmWave D2D.

Another interesting observation is that higher obstacle densities lead to higher coverage probabilities at high SINR thresholds. In other words, obstacles can help control/manage interference in mmWave networks to improve network performance.

2) *D2D Link Coverage*: The coverage probabilities for mmWave and microwave D2D links, obtained analytically from (18) (Theorem 2) and (20) (Theorem 3), respectively, are shown in Fig. 5 with respect to the SINR threshold and compared against PPP-based model simulations. For mmWave D2D links, the analytical results obtained by dominant interferer analysis provide a significantly tighter upper bound on the PPP-based model simulations than for mmWave cellular links. This is because the relatively lower antenna heights of D2D transmitters and receivers result in more blockages and less interference from distant interferers. For microwave D2D links, the analytical results closely align with the PPP-based model simulations.

Comparing the two D2D communications options, we observe that microwave D2D performs better than mmWave D2D in the UMa scenario. This is because microwave D2D links can be established under NLOS conditions, whereas mmWave D2D links can only be established under LOS conditions. However, microwave D2D links perform much worse than mmWave D2D links in the Ind scenario. This is because the dense BS deployment and fully utilized resources in each cell ($\rho = 1$) lead to severe interference in the uplink microwave spectrum. In contrast, mmWave D2D links experience less interference due to blockages and because the antenna arrays reject interference from off-boresight directions. Evidently, microwave D2D is a worse

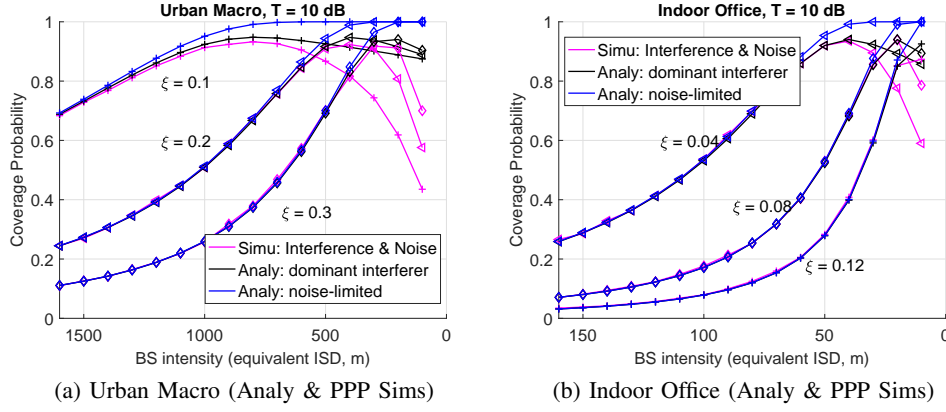


Fig. 6: Validation of the coverage expression in (19) (Corollary 1) for noise-limited mmWave cellular links against the PPP-based model simulations. MmWave cellular links are noise-limited at low BS densities/high ISDs and are interference-limited at high BS densities/low ISDs. Dominant interference analysis fails at high BS densities/low ISDs. Moreover, for mmWave cellular communications, there is an optimal BS density that increases with the obstacle density.

choice for extremely dense BS deployments.

C. Noise-Limited MmWave Link Coverage

In this section, we study the mmWave cellular link coverage probability under the noise-limited assumption. We will compare the analytical results calculated according to (19) (Corollary 1) with PPP-based model simulation results to determine if we can ignore interference on mmWave links. In the simulations, both interference and noise are taken into account.

The coverage probabilities for noise-limited mmWave cellular links, obtained analytically from (19) (Corollary 1), are shown in Fig. 6 with respect to the BS intensity. The noise-limited analytical results are compared against the analytical results obtained by dominant interferer analysis and PPP-based model simulations considering both interference and noise. Note that the urban macro [Fig. 6(a)] and indoor office [Fig. 6(b)] scenarios are based on the 3GPP UMa and Ind scenarios, respectively, with parameter configurations in Table II, but with variations in the BS and obstacle densities. Here, we fix the outage SINR threshold to $T = 10$ dB and express the BS density through the equivalent ISD.

In both scenarios, the mmWave cellular link is noise-limited at low BS densities/high ISDs and interference-limited at high BS densities/low ISDs. We observe that for each obstacle density, there is an effective ISD *threshold* below which the network tends to be interference-limited (for example, for $\xi = 0.1$ in the urban macro scenario and $\xi = 0.04$ in the indoor office scenario,

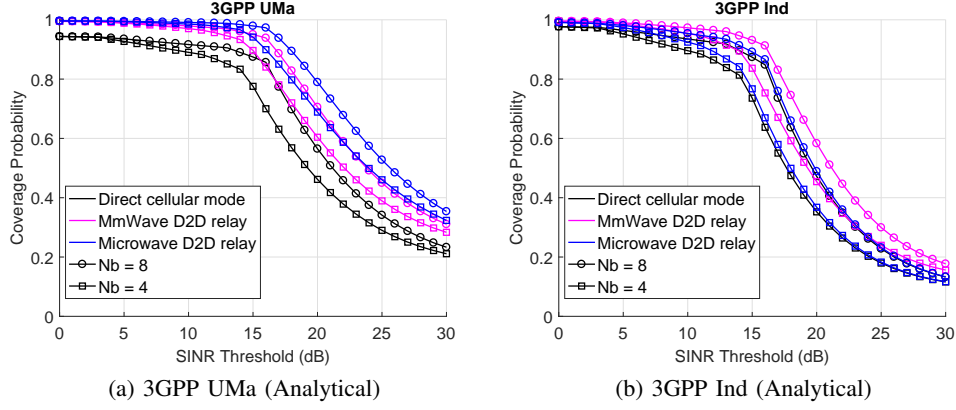


Fig. 7: Coverage improvement of a D2D relay-assisted mmWave cellular network.

ISDs below 700 m and 40 m, respectively, start to demonstrate interference-limited behavior). Furthermore, this BS density threshold increases with the obstacle density. We also observe that dominant interferer analysis becomes inaccurate at extreme BS densities/very small ISDs due to the increase in interference in extremely dense mmWave BS deployments.

D. Coverage Improvement Enabled by D2D Relaying in MmWave Cellular Networks

Now that the coverage probability expressions for the cellular and D2D links have been validated, we can calculate the coverage probabilities in D2D relay-assisted mmWave cellular networks using (13).

1) *Coverage Improvement in 3GPP Scenarios:* The coverage probabilities for a D2D relay-assisted mmWave cellular network, obtained analytically by substituting (17) and (18) (for mmWave D2D links), or (17) and (20) (for microwave D2D links), into (13) are shown in Fig. 7 with respect to the SINR threshold. We note that D2D relays improve the coverage in both UMa and Ind scenarios, with larger gains in the UMa scenario due to the larger transmit distances.

2) *Coverage vs. BS/Obstacle Density:* The coverage probabilities for a D2D relay-assisted mmWave cellular network, obtained analytically as above, are shown in Fig. 8 with respect to the BS intensity. Note that the urban macro and indoor office scenarios are the same as in Section IV-C. Also note that candidate relay UE intensities are fixed in a given scenario (urban macro or indoor office).

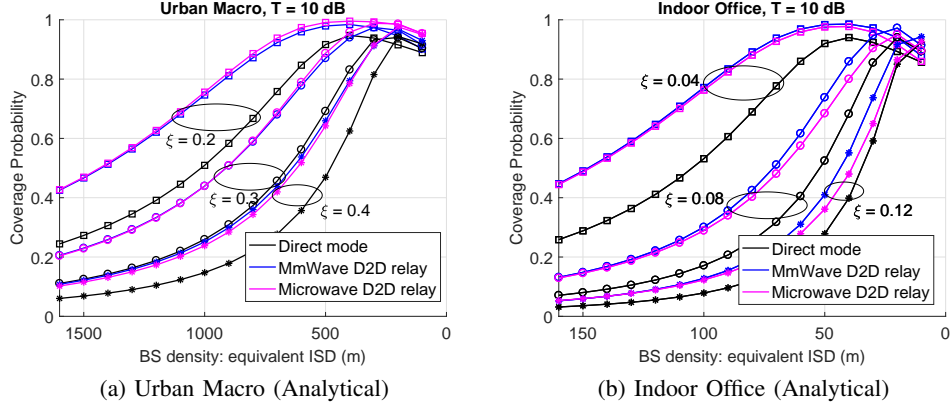


Fig. 8: Coverage improvement in a relay-assisted mmWave cellular network. There is an optimal BS deployment density, which increases with the obstacle coverage ratio.

We observe that D2D relays improve the coverage for all BS densities for the selected SINR threshold $T = 10$ dB. We also observe that, given a specific obstacle cover ratio, there is an optimal BS deployment density in D2D relay-assisted mmWave cellular networks, which increases with the obstacle cover ratio.

V. CONCLUSION

We envision mmWave cellular networks in which D2D relays are used to route around blockages. Using stochastic geometry, we derived a coverage probability model for the downlink of a D2D relay-assisted mmWave cellular network under the assumption that the coverage probabilities of cellular and D2D links are independent. For mmWave links, we derive the coverage probability using dominant interferer analysis while accounting for blockages and beamforming gains. For microwave D2D links, we derive the coverage probability using different path loss models for LOS and NLOS links. Our analytical and simulation results provide numerous important insights on the coverage of mmWave cellular links, mmWave D2D links, microwave D2D links, and D2D relay-assisted mmWave cellular networks:

- Dominant interferer analysis provides a tight upper bound on the coverage probabilities obtained by PPP-based model simulations for both mmWave cellular links and mmWave D2D links because the effective number of distant interferers is reduced by both blockages and beamforming gains. The upper bound is tighter for higher obstacle densities and for D2D links because they experience higher obstacle densities than cellular links. Dominant

interferer analysis becomes inaccurate at extremely high BS densities/low ISDs, particularly when the obstacle density is low.

- Obstacles play an important role in mitigating interference on mmWave cellular links and mmWave D2D links. On mmWave cellular links, higher obstacle densities lead to higher coverage probabilities at high SINR thresholds. On mmWave D2D links, blockages significantly reduce interference in dense BS deployments with fully utilized resources in each cell. In contrast, microwave D2D links experience poor coverage in these conditions.
- MmWave cellular links are noise-limited at light to moderate BS densities, but become interference-limited at higher BS densities.
- The BS density that maximizes the coverage probability increases with the obstacle density in both mmWave cellular networks and relay-assisted mmWave cellular networks.
- MmWave and microwave D2D relays improve the downlink coverage probability in urban macro and indoor office scenarios across a wide range of BS densities and SINR thresholds.

Future work should investigate: (i) The benefits of D2D relay-assisted communications on the uplink of mmWave cellular networks. This will be challenging because, assuming D2D links reuse uplink spectrum, the interference on the cellular and D2D links will be correlated. (ii) The correlation of blockages experienced by cellular and D2D links when setting up D2D relay transmissions. (iii) The spectral efficiency when using mmWave and microwave D2D relays.

APPENDIX A

PROOF OF LEMMA 2

As assumed, only LOS transmitters are interested and thus we remove the candidate transmitters that do not have LOS path to a destination UE. To achieve this, the so-called $p(\mathbf{x})$ -thinning is performed: a point with coordinates \mathbf{x} is removed from a parent PPP with probability $1 - p(\mathbf{x})$ (or, a point is retained with probability $p(\mathbf{x})$) [22]. Here transmitters with NLOS path will be removed, so the retaining probability of a transmitter d_i away from the typical UE is exactly the LOS probability $p_L(d_i)$.

By thinning theory, the retained points form an inhomogeneous PPP. The average number of transmitters with LOS path to the typical UE falling into the disc $B(\mathbf{o}, d)$ centered the typical

UE with radius d is

$$\Lambda(d, \lambda) = \int_{B(\mathbf{o}, d)} p(\mathbf{x}) \lambda(d\mathbf{x}) = \int_0^{2\pi} \int_0^d p_L(x) \lambda x dx d\theta = \frac{2\pi\lambda c}{\beta^2} (1 - e^{-\beta d} - \beta d e^{-\beta d}).$$

Therefore, the cumulative distribution function (CDF) of d_0 is

$$F_{d_{0,L}}(d) = \mathbb{P}[d_{0,L} < d] = 1 - \mathbb{P}[d_{0,L} \geq d] = 1 - \exp(-\Lambda(d, \lambda));$$

and thus the PDF of d_0 is derived as

$$f_{d_{0,L}}(d) = \frac{dF_{d_{0,L}}(d)}{dd} = 2\pi\lambda c d e^{-\Lambda(d, \lambda) - \beta d}.$$

APPENDIX B

PROOF OF THEOREM 1

In order to investigate the outage caused by interference, we only need to study the point process of LOS interferers in the IR; non-desired BSs that don't have LOS path to the typical receiver will be removed similarly by $p(\mathbf{x})$ -thinning. For interferers in FIR, moreover, the retained LOS interferers shall be thinned further since only LOS interferers with main lobe towards the typical receiver matter: a LOS BS will be retained as a dominant interferer with probability $\frac{\phi_b}{2\pi}$.

By thinning theory, given the distance d_0 between the typical UE and its nearest LOS BS, the average number of dominant LOS BS falling into the NIR is

$$\begin{aligned} \Lambda_b^{(N)}(T, d_0) &= \int_{\text{NIR}} p(\mathbf{x}) \lambda_b(d\mathbf{x}) \\ &= \int_0^{\phi_u} \int_{d_0}^{D_3} p_L(x) \lambda_b x dx d\theta + \int_{\phi_u}^{2\pi} \int_{d_0}^{D_1} p_L(x) \lambda_b x dx d\theta \\ &= \frac{\lambda_b c}{\beta^2} \left(\phi_u (\beta d_0 e^{-\beta d_0} - \beta D_3 e^{-\beta D_3} + e^{-\beta d_0} - e^{-\beta D_3}) \right. \\ &\quad \left. + (2\pi - \phi_u) (\beta d_0 e^{-\beta d_0} - \beta D_1 e^{-\beta D_1} + e^{-\beta d_0} - e^{-\beta D_1}) \right). \end{aligned}$$

Average number of dominant LOS BS falling into the FIR can be obtained similarly. Note that

for FIR, only the BSs with boresight towards typical UE will be retained. We have

$$\begin{aligned}
\Lambda_b^{(F)}(T, d_0) &= \frac{\phi_b}{2\pi} \int_{\text{FIR}} p(\mathbf{x}) \lambda_b(d\mathbf{x}) \\
&= \frac{\phi_b}{2\pi} \left(\int_0^{\phi_u} \int_{D_3}^{D_4} p_L(x) \lambda_b x dx d\theta + \int_{\phi_u}^{2\pi} \int_{D_1}^{D_2} p_L(x) \lambda_b x dx d\theta \right) \\
&= \frac{\phi_b \lambda_b c}{2\pi \beta^2} \left(\phi_u (\beta D_3 e^{-\beta D_3} - \beta D_4 e^{-\beta D_4} + e^{-\beta D_3} - e^{-\beta D_4}) \right. \\
&\quad \left. + (2\pi - \phi_u) (\beta D_1 e^{-\beta D_1} - \beta D_2 e^{-\beta D_2} + e^{-\beta D_1} - e^{-\beta D_2}) \right).
\end{aligned}$$

Obviously, the coverage probability by dominant interferer analysis is the null probability, i.e. no retained interferer (BS) falls into both the NIR and FIR. For given outage SINR threshold T , we have $p_c(T, d_0) = e^{-\Lambda_b^{(N)}(T, d_0) - \Lambda_b^{(F)}(T, d_0)}$, the coverage probability for a typical UE is

$$\begin{aligned}
p_c(T) &= \mathbb{E}_{d_0} [p_c(T, d_0)] \\
&= \int_{x>0} p_c(T, x) f_{d_0}(x) dx \\
&= 2\pi \lambda_b c \int_{x>0} x e^{-\Lambda_b^{(N)}(T, x) - \Lambda_b^{(F)}(T, x) - \Lambda(x, \lambda_b) - \beta x} dx.
\end{aligned}$$

APPENDIX C

PROOF OF THEOREM 3

Denote $d_{0,N}$ and $d_{0,L}$ the distances from the typical UE to its nearest NLOS candidate relay UE and nearest LOS candidate relay UE. The nearest NLOS candidate relay UE will be selected as relay if $A_L^{-1} d_{0,L}^{-\alpha_L} < A_N^{-1} d_{0,N}^{-\alpha_N}$. For $\lambda_{cr} > 0$, we have

$$\begin{aligned}
\mathbb{P}(A_L^{-1} d_{0,L}^{-\alpha_L} < A_N^{-1} d_{0,N}^{-\alpha_N}) &= \mathbb{P}(d_{0,N} < \tilde{a} d_{0,L}^{\alpha_L/\alpha_N}) \\
&= \int_0^\infty f_{d_{0,L}}(x) \int_0^{\tilde{a} x^{\alpha_L/\alpha_N}} f_{d_{0,N}}(y) dy dx \\
&= \int_0^\infty f_{d_{0,L}}(x) F_{d_{0,N}}(\tilde{a} x^{\frac{\alpha_L}{\alpha_N}}) dx \\
&= 1 - \int_0^\infty f_{d_{0,L}}(x) e^{-\pi \lambda_{cr} \tilde{a}^2 x^2 \frac{\alpha_L}{\alpha_N} + \Lambda(\tilde{a} x^{\frac{\alpha_L}{\alpha_N}}, \lambda_{cr})} dx \\
&= 1 - 2\pi \lambda_{cr} c \int_0^\infty x e^{-\Lambda(x, \lambda_{cr}) - \beta x - \pi \lambda_{cr} \tilde{a}^2 x^2 \frac{\alpha_L}{\alpha_N} + \Lambda(\tilde{a} x^{\frac{\alpha_L}{\alpha_N}}, \lambda_{cr})} dx \\
&\triangleq S_N,
\end{aligned} \tag{25}$$

where $\Lambda(d, \lambda)$ is given as (11). S_N here is defined as the probability that UE associates to a LOS candidate relay UE. Similarly we can obtain S_L , the probability that UE associates to a NLOS

candidate relay UE, and $S_L + S_N = 1$.

The coverage probability of D2D link, given that the D2D link is NLOS (or, UE associates to the nearest NLOS candidate relay UE) and has length $d_{0,N}$, is

$$\begin{aligned}
p_{c,N}(T, d_{0,N}) &= \mathbb{P}[\text{SINR} > T] \\
&= \mathbb{P}\left[\frac{h A_N^{-1} d_{0,N}^{-\alpha_N}}{\sigma^2 + I} > T\right] \\
&= \mathbb{E}_I[\mathbb{P}[h > T A_N d_{0,N}^{\alpha_N}(\sigma^2 + I) | I]] \\
&\stackrel{(a)}{=} \mathbb{E}_I[e^{-T A_N d_{0,N}^{\alpha_N}(\sigma^2 + I)}] \\
&= e^{-T A_N d_{0,N}^{\alpha_N} \sigma^2} \mathcal{L}_I(T A_N d_{0,N}^{\alpha_N}),
\end{aligned} \tag{26}$$

where (a) follows the fact that $h_N \sim \exp(\mu)$ and we assume $\mu = 1$; $\mathcal{L}_I(\cdot)$ denotes Laplace transform of interference I . With the assumption of Rayleigh fading interference, we have [25]

$$\mathcal{L}_I(s) = \exp\left(-\pi \rho \lambda_b s^{2/\alpha_N} \frac{2\pi/\alpha_N}{\sin(2\pi/\alpha_N)}\right).$$

Note that the path loss exponent of interference links is assumed to be α_N . Now we have

$$\begin{aligned}
p_{c,N}(T) &= \mathbb{E}_{d_{0,N}}[p_{c,N}(T, d_{0,N})] \\
&= \int_{x>0} p_{c,N}(T, x) f_{d_{0,N}}(x) dx \\
&= 2\pi \lambda_{cr} \int_0^\infty x(1 - ce^{-\beta x}) e^{\Lambda(x, \lambda_{cr}) - \pi \lambda_{cr} x^2 - T \sigma^2 A_N x^{\alpha_N}} \mathcal{L}_I(T A_N x^{\alpha_N}) dx.
\end{aligned} \tag{27}$$

When the nearest LOS candidate relay UE is selected as relay, i.e. $d_{0,N}^{-\alpha_N} \geq d_{0,L}^{-\alpha_L}$, similarly, we have $p_{c,L}(T, d_{0,L}) = e^{-T A_L d_{0,L}^{\alpha_L} \sigma^2} \mathcal{L}_I(T A_L d_{0,L}^{\alpha_L})$, and

$$\begin{aligned}
p_{c,L}(T) &= \mathbb{E}_{d_{0,L}}[p_{c,L}(T, d_{0,L})] \\
&= \int_{x>0} p_{c,L}(T, x) f_{d_{0,L}}(x) dx \\
&= 2\pi \lambda_{cr} \int_{x>0} e^{-\Lambda(x, \lambda_{cr}) - \beta x - T \sigma^2 A_L x^{\alpha_L}} \mathcal{L}_I(T A_L x^{\alpha_L}) dx.
\end{aligned} \tag{28}$$

By total probability law, the microwave D2D link coverage probability for given SINR threshold T is $p_c(T) = S_N p_{c,N}(T) + S_L p_{c,L}(T)$. We thus complete the proof.

REFERENCES

- [1] T. S. Rappaport, S. Sun, R. Mayzus, H. Zhao, Y. Azar, K. Wang, G. N. Wong, J. K. Schulz, M. Samimi, and F. Gutierrez, "Millimeter wave mobile communications for 5g cellular: it will work!" *IEEE Access*, vol. 1, pp. 335-349, May 2013.
- [2] 3GPP, "Technical report 38.900: Channel model for frequency spectrum above 6 GHz (Release 14)" v14.1.0. Sept. 2016. [Online]. Available: <http://www.3gpp.org/DynaReport/38900.htm>
- [3] Federal Communications Commission (FCC), "Spectrum frontiers R&O and FNPRM," July 2016. [Online]. Available: <https://www.fcc.gov/document/spectrum-frontiers-ro-and-fnprm>
- [4] H. Zhao, *et al.*, "28 GHz millimeter wave cellular communication measurements for reflection and penetration loss in and around buildings in New York City," in *Proc. IEEE ICC*, 2013, pp. 5163-5167.
- [5] S. Collonge, G. Zaharia, and G. E. Zein, "Influence of human activity on wide-band characteristics of the 60GHz indoor radio channel," *IEEE Trans. Wireless Commun.*, vol. 3, no. 6, pp. 2369-2406, Nov. 2004.
- [6] T. S. Rappaport, *et al.*, "Broadband millimeter-wave propagation measurements and models using adaptive-beam antennas for outdoor urban cellular communications," *IEEE Trans. Antennas and Propag.*, vol. 61, no. 4, pp. 1850-1859, Apr. 2013.
- [7] Y. Niu, Y. Li, D. Jin, L. Su, A. V. Vasilakos, "A survey of millimeter wave (mmWave) communications for 5G: opportunities and challenges," ArXiv e-print, Feb. 2015. [Online]. Available: <http://arxiv.org/abs/1502.07228>
- [8] 3GPP, "Technical specification 36.216: Physical layer for relaying operation", v13.0.0. Jan. 2016.
- [9] C. Hoymann, *et al.*, "Relaying operation in 3GPP LTE: challenges and solutions," *IEEE Commun. Mag.*, vol. 50, issue 2, pp. 156-162, Feb. 2012.
- [10] Wi-Fi Alliance, "Wi-fi direct," [Online]. Available: <http://www.wi-fi.org/discover-wi-fi/wi-fi-direct>
- [11] Qualcomm, "Lte direct," [Online]. Available: <https://www.qualcomm.com/invention/research/projects/lte-direct>
- [12] D. Feng, L. Lu, Y. Yuan-Wu, G. Li, S. Li, and G. Feng, "Device-to-device communications in cellular networks," *IEEE Commun. Mag.*, vol. 52, no. 4, pp. 4955, 2014.
- [13] 3GPP, RP-142311: "Work Item Proposal for Enhanced LTE Device to Device Proximity Services," Dec. 2014.
- [14] X. Wu, S. Tavildar, S. Shakkottai, T. Richardson, J. Li, R. Laroia, and A. Jovicic, FlashLinQ: A Synchronous Distributed Scheduler for Peer-to-Peer Ad Hoc Networks, *IEEE/ACM Trans. on Networking*, vol. 21, no. 4, pp. 1215-1228, August 2013.
- [15] N. Golrezaei, A. F. Molisch, A. G. Dimakis, and G. Caire, Femtocaching and device-to-device collaboration: A new architecture for wireless video distribution, *IEEE Commun. Mag.*, vol. 51, no. 4, pp. 1421-149, 2013.
- [16] M. S. Corson, R. Laroia, J. Li, V. Park, T. Richardson, and G. Tsirtsis, "Toward proximity-aware internetworking," *IEEE Wireless Commun.*, vol. 17, no. 6, pp. 2633, December 2010.
- [17] B. Zhou, H. Hu, S.-Q. Huang, and H.-H. Chen, Intracell device-to-device relay algorithm with optimal resource utilization, *IEEE Trans. on Vehicular Technology*, vol. 62, no. 5, pp. 2315-2326, Jun 2013.
- [18] N. K. Pratas and P. Popovski, Underlay of low-rate machine-type D2D links on downlink cellular links, in *2014 IEEE International Conference on Communications (ICC)*, June 2014.
- [19] N. Mastrorade, V. Patel, J. Xu, L. Liu, and M. van der Shaar, "To relay or not to relay: learning device-to-device relaying strategies in cellular networks," *IEEE Trans. Mobile Computing*, vol. 15, issue 6, pp. 1569-1585, Jan. 2016.
- [20] W. Roh, *et al.*, "Millimeter-wave beamforming as an enabling technology for 5G cellular communications: theoretical feasibility and prototype results," *IEEE Commun. Mag.*, vol. 52, issue 2, pp. 106-113. Feb. 2014.
- [21] K. Venugopal, M. C. Valenti, and R. W. Heath, Jr., "Interference in finite-sized highly dense millimeter wave networks," in *Proc. IEEE Inf. Theory Appl. Workshop (ITA)*, pp. 175-180. Feb. 2015.

- [22] S. Chiu, D. Stoyan, W. Kendall, and J. Mecke, *Stochastic Geometry and Its Applications*, 3rd edition. Wiley, 2013.
- [23] F. Baccelli and B. Blaszczyzyn, *Stochastic Geometry and Wireless Networks, Volume I-Theory*. Delft, The Netherlands: NOW, 2009.
- [24] J. G. Andrews, F. Baccelli, and R. Krishna Ganti, "A tractable approach to coverage and rate in cellular networks," *IEEE Trans. Commun.*, vol. 59, no. 11, pp. 3122-3134, Nov. 2011.
- [25] M. Haenggi, *et al.*, "Stochastic geometry and random graphs for the analysis and design of wireless networks," *IEEE J. Sel. Areas Commun.*, vol. 27, no. 7, pp. 1029-1046, Aug. 2009.
- [26] J. Qiao, *et al.*, "Enabling device-to-device communications in millimeter-wave 5G cellular networks," *IEEE Commun. Mag.*, vol. 53, issue 1, pp. 209-215, Jan. 2015.
- [27] X. Lin and J. G. Andrews, "Connectivity of millimeter wave networks with multi-hop relaying," *IEEE Wireless Commun. Letters*, vol.4, no. 2, pp. 209-212, Apr. 2015.
- [28] N. Wei, X. Lin, and Z. Zhang, "Optimal relay probing in millimeter wave cellular systems with device-to-device relaying," *IEEE Trans. Vehicular Technology*, vol. PP, issue 99, pp. 1-6, Apr. 2016.
- [29] T. Bai, R. Vaze, and R. Heath, "Analysis of blockage effects on urban cellular networks," *IEEE Trans. on Wireless Commun.*, vol. 13, no. 9, pp. 5070-5083, Sept. 2014.
- [30] C. H. Lee, C. Y. Shih, and Y. S. Chen, "Stochastic geometry based models for modeling cellular networks in urban areas," *Wireless Networks*, vol. 19, issue 6, pp. 1063-1072, Aug. 2013.
- [31] IEEE Standard for Information technology, "Wireless LAN Medium Access Control (MAC) and Physical Layer (PHY) Specifications Amendment 3: Enhancements for Very High Throughput in the 60 GHz Band," IEEE 802.11ad, Dec. 2012.
- [32] 3GPP, "Technical Specification 36.300: Evolved Universal Terrestrial Radio Access Network (E-UTRAN); Overall description (Release 13)," v13.4.0. June 2016. [Online]. Available: <http://www.3gpp.org/DynaReport/36300.htm>
- [33] X. Lin, J. G. Andrews, A. Ghosh, and R. Ratasuk, "An overview of 3GPP device-to-device proximity services," *IEEE Commun. Mag.*, vol. 52, issue 4, pp. 40-48, Apr. 2014.
- [34] S. Weber, J. G. Andrews, and N. Jindal, "An overview of the transmission capacity of wireless networks," *IEEE Trans. Commun.*, vol. 58, no. 12, pp. 3593-3604, Dec. 2010.
- [35] S. Rangan, T. S. Rappaport, and E. Erkip, "Millimeter wave cellular wireless networks: potentials and challenges," *Proc. IEEE*, vol. 102, no. 3, pp. 366-385, Mar. 2014.
- [36] M. R. Akdeniz *et al.*, "Millimeter wave channel modeling and cellular capacity evaluation," *IEEE J. Sel. Areas Commun.*, vol. 32, no. 6, pp. 1164-1179, June 2014.
- [37] T. Bai, and R. W. Heath Jr., "Coverage and rate analysis for millimeter-wave cellular networks," *IEEE Trans. Wireless Commun.*, vol. 14, no. 2, pp. 1100-1114, Aug. 2014.
- [38] 3GPP, "Technical report 36.814: Further advancements for E-UTRA physical layer aspects," v9.0.0. Mar. 2010. [Online]. Available: <http://www.3gpp.org/dynareport/36814.htm>
- [39] 3GPP, "Technical report 36.843: Study on LTE device to device proximity services; radio aspects," v12.0.1. Mar. 2014. [Online]. Available: <http://www.3gpp.org/dynareport/36843.htm>